PNAS RESEARCH ARTICLE | IMMUNOLOGY AND INFLAMMATION

TLR priming licenses NAIP inflammasome activation by immunoevasive ligands

James P. Grayczyk[a,1,2], Luying Liu[a,1], Marisa S. Egan[b], Emily Aunins[a], Meghan A. Wynosky-Dolfi[a,3], Scott W. Canna[c], Andy J. Minn[d,e,f,g], Sunny Shin[b,4], and Igor E. Brodsky[a,4]

Affiliations are included on p. 11.

Edited by Vishva Dixit, Genentech, South San Francisco, CA; received July 12, 2024; accepted August 14, 2024

NLR family, apoptosis inhibitory proteins (NAIPs) detect bacterial flagellin and structurally related components of bacterial type III secretion systems (T3SS), and recruit NLR family CARD domain containing protein 4 (NLRC4) and caspase-1 into an inflammasome complex that induces pyroptosis. NAIP/NLRC4 inflammasome assembly is initiated by the binding of a single NAIP to its cognate ligand, but a subset of bacterial flagellins or T3SS structural proteins are thought to evade NAIP/NLRC4 inflammasome sensing by not binding to their cognate NAIPs. Unlike other inflammasome components such as NLRP3, AIM2, or some NAIPs, NLRC4 is constitutively present in resting macrophages and not known to be induced by inflammatory signals. Here, we demonstrate that Toll-like receptor (TLR)-dependent p38 mitogen-activated protein kinase signaling up-regulates NLRC4 transcription and protein expression in murine macrophages, which licenses NAIP detection of evasive ligands. In contrast, TLR priming in human macrophages did not up-regulate NLRC4 expression, and human macrophages remained unable to detect NAIP-evasive ligands even following priming. Critically, ectopic expression of either murine or human NLRC4 was sufficient to induce pyroptosis in response to immunoevasive NAIP ligands, indicating that increased levels of NLRC4 enable the NAIP/NLRC4 inflammasome to detect these normally evasive ligands. Altogether, our data reveal that TLR priming tunes the threshold for the murine NAIP/NLRC4 inflammasome to enable inflammasome responses against immunoevasive or suboptimal NAIP ligands. These findings provide insight into species-specific TLR regulation of NAIP/NLRC4 inflammasome activation.

Inflammasome | NLRC4 | pyroptosis | Type III secretion | NAIP

Pattern recognition receptors (PRRs) sense pathogen-associated molecular patterns (PAMPs) and signatures of pathogenesis during bacterial infection and promote innate immune responses to clear infection (1–3). Many gram-negative bacterial pathogens encode type III secretion systems (T3SS) to deliver effector proteins into host cells and use the motility organelle flagella to promote infection. However, in addition to effector proteins, the T3SS of many pathogens translocate flagellin as well as structural components of the T3SS apparatus into the host cell cytosol (4). The NLR family apoptosis inhibitor proteins (NAIPs) bind to cytosolic flagellin and T3SS components, resulting in assembly of a multimeric protein complex known as the inflammasome that plays a crucial role in host defense against bacterial infections (5–7).

In mice, NAIP5 and NAIP6 detect cytosolic flagellin of bacterial pathogens such as *Salmonella*, *Legionella*, and *Pseudomonas*, while NAIP1 and NAIP2 recognize portions of the T3SS termed the needle and inner rod subunits, respectively (6–13). In contrast, humans encode a single NAIP that broadly recognizes all three types of ligands (14–17). Upon binding to their cognate ligands, NAIPs recruit nucleotide-binding domain, leucine-rich repeat-containing protein caspase recruitment domain containing protein 4 (NLRC4), which in turn recruits and activates the zymogen protease caspase 1 (Casp1) to form the NAIP/NLRC4 inflammasome (14, 15, 18–23). Active Casp1 in turn cleaves the proform of interleukin (IL)-1 family cytokines IL-1β and IL-18, as well as the pore-forming protein gasdermin D (GSDMD) to mediate pyroptosis (24–26).

The NAIP/NLRC4 inflammasome serves as an important barrier to bacterial colonization and infection. Notably, *Salmonella enterica* serovar Typhimurium (*S.* Tm) down-regulates flagellin expression during its systemic phase, which is important for evasion of NLRC4-mediated host defense (27–31). Moreover, genetic resistance to *Legionella* infection in inbred mice is dependent on a functional *Naip5* gene, and *Legionella* expressing flagellin are rapidly cleared in a NAIP5/NLRC4-dependent manner (9, 12, 22). Additionally, wild-type mice are resistant to colonization by the primate-specific enteric pathogen, *Shigella flexneri*, whereas *Nlrc4*$^{-/-}$ mice are highly susceptible (32, 33).

Significance

Cytosolic receptors of the neuronal apoptosis inhibitor protein (NAIP) family detect bacterial flagellin and components of the type III secretion system (T3SS). NAIPs binding their cognate ligand recruits NLR family, Caspase activation and recruitment domain (CARD) containing protein 4 (NLRC4) to form NAIP/NLRC4 inflammasomes, culminating in pyroptosis. However, some bacterial pathogens evade NAIP/NLRC4 inflammasome detection, thus bypassing a crucial innate immune barrier. Here, we find that murine macrophage Toll-like receptor (TLR)-dependent p38 mitogen-activated protein kinase (MAPK) signaling increases NLRC4 expression, thereby lowering the threshold for NAIP/NLRC4 inflammasome activation by immunoevasive NAIP ligands. Human macrophages were unable to undergo priming-induced upregulation of NLRC4 and could not detect immunoevasive NAIP ligands. These findings provide insight into species-specific regulation of the NAIP/NLRC4 inflammasome.

The authors declare no competing interest.

This article is a PNAS Direct Submission.

[1]J.P.G. and L.L. contributed equally to this work.

[2]Present address: Oncology Discovery Research, AbbVieInc., North Chicago, IL 60064.

[3]Present address: Immunology Research Unit, GlaxoSmithKline, Collegeville, PA 19426.

[4]To whom correspondence may be addressed. Email: sunshin@pennmedicine.upenn.edu or ibrodsky@vet.upenn.edu.

This article contains supporting information online at https://www.pnas.org/lookup/suppl/doi:10.1073/pnas.2412700121/-/DCSupplemental.

Published November 18, 2024.

NAIP5 binds to the flagellin D0 domain, which consists of N- and C-terminal alpha-helical regions (34, 35). Notably, the C-terminal 35 amino acids of the D0 domain are both necessary and sufficient for NAIP5/NLRC4 activation (36). Importantly, a small number of key residues at the C terminus distinguish between closely related flagellins that activate or do not activate NAIP/NLRC4 inflammasomes. Specifically, activating flagellins from *S.* Tm, *Legionella*, or *Pseudomonas* all possess a C-terminal arginine. In contrast, flagellins that are reported to be poor activators of the NAIP/NLRC4 inflammasome from *Helicobacter pylori*, enteropathogenic *Escherichia coli* (EPEC), *Burkholderia thailandensis*, and several commensal bacteria lack this C-terminal arginine and instead contain C-terminal glutamine, glutamine-glycine, or threonine residues (7, 37, 38). These flagellins also do not bind NAIP5 in yeast two-hybrid assays (7), implying that NAIP binding determines activation of the NAIP/NLRC4 inflammasome. Indeed, structural studies indicate that NAIP5/NLRC4 inflammasome assembly is initiated by a single flagellin binding a single NAIP, leading to recruitment and polymerization of NLRC4 subunits and formation of the inflammasome (19, 21, 35, 37, 39).

In contrast to inflammasome sensor proteins such as NLRP3, AIM2, and NAIP1 (11, 40, 41), adaptor proteins such as NLRC4 are not widely considered to be transcriptionally induced in response to inflammatory signals, beyond a role for the transcription factors interferon regulatory factor 8 (IRF8) and bromodomain-containing protein 4 (BRD4) in basal expression of *Nlrc4* and the *Naips* (42, 43). Whether inflammatory signals regulate NLRC4 expression and the potential consequences of such regulation on NAIP/NLRC4 inflammasome function is not known. Here, we find that TLR priming enables NAIP/NLRC4 detection of EPEC flagellin, which is normally not sensed in the absence of such priming. TLR stimulation up-regulated NLRC4 expression, which correlated with enhanced NAIP/NLRC4 inflammasome-dependent responses. This enhanced NAIP/NLRC4 response required MyD88 and p38 mitogen-activated protein kinase (MAPK) signaling, as well as NAIP5. Notably, TLR priming licensed NLRC4-dependent inflammasome responses to other evasive NAIP ligands, including the *S.* Tm *Salmonella* pathogenicity island 2 (SPI-2) inner rod and needle proteins, indicating that TLR priming lowers the threshold for NAIP/NLRC4 inflammasome activation in response to immunoevasive NAIP ligands. Interestingly, *S. enterica* serovar Typhimurium expressing immunoevasive flagellin induced lower levels of IL-18 in serum following acute infection. Surprisingly, we found that NLRC4 was not up-regulated in TLR-primed human macrophages, correlating with lack of responsiveness by human macrophages to immunoevasive flagellins. Ectopic expression of murine or human NLRC4 in murine or human macrophages conferred enhanced inflammasome responses against immunoevasive flagellin, indicating that NLRC4 expression levels regulate responses to suboptimal NAIP ligands. Our findings reveal that TLR priming licenses the NAIP-NLRC4 inflammasome detection of immunoevasive NAIP ligands by increasing NLRC4 expression. Furthermore, we uncover a key distinction between the ability of human and murine NAIP/NLRC4 inflammasomes to respond to immunoevasive NAIP ligands.

Results

C-Terminal Glutamine Residues in Flagellin Disable Recognition by the NAIP/NLRC4 Inflammasome. Retroviral transduction, protein transfection, anthrax toxin-based delivery, and *L. monocytogenes* ActA-fusion proteins have all been utilized as approaches to deliver NAIP ligands into host cells (10, 11, 13, 16, 17, 35, 36, 44). However, cytosolic delivery of flagellin, T3SS inner rod, or T3SS needle proteins naturally occurs via translocation through a T3SS or T4SS itself (4). We therefore sought to develop an alternative method to deliver flagellin into the cell in order to study mechanisms of NAIP/NLRC4 inflammasome activation in response to T3SS-based delivery of NAIP ligands. Specifically, we developed a heterologous delivery system using the T3SS of the enteric gram-negative pathogen *Yersinia pseudotuberculosis* (*Yp*) by fusing the C-terminal FliCD0 region of flagellin to the N-terminal 100 amino acids of the T3SS-secreted *Yersinia* outer protein E ($YopE^{1-100}$), which contains the YopE N-terminal secretion and translocation signal (*SI Appendix*, Fig. *S*1). *Yp* represses expression of its own flagella during infection, allowing us to avoid any inflammatory responses by *Yp* flagella (45, 46). We also used *Yp* on a Δ*yopJ* background to prevent activation of YopJ-induced cell death (47–49). As expected, Δ*yopJ Yp* expressing *S.* Tm FliCD0 YopE fusion (FliCD0), but not EPEC FliCD0 YopE fusion (EPEC FliCD0) or the first 100 amino acids of YopE alone ($YopE^{1-100}$), induced significant cell death of bone marrow–derived macrophages (BMDMs) in an NLRC4- and Casp1/11-dependent manner (Fig. 1*A*). Consistently, delivery of *S.* Tm FliCD0 but not of EPEC FliCD0 or $YopE^{1-100}$ induced IL-1β release and cleavage of both Casp1 and GSDMD, which are markers of pyroptosis (Fig. 1 *B* and *C*). Similar levels of *S.* Tm FliCD0 and EPEC FliCD0 were expressed and secreted by *Yp* (*SI Appendix*, Fig. S1*B*), demonstrating that the observed difference in cell death and pyroptotic markers is not due to poor expression or secretion of the EPEC FliCD0 fusion protein.

Three conserved leucine residues at the C terminus of flagellin confer binding by NAIP5 and subsequent activation of the NAIP5/NLRC4 inflammasome (36). However, these leucines are retained in flagellins from bacteria such as *E. coli* that do not activate the inflammasome, indicating that other residues are likely important for NAIP5 binding. Recent studies employing ectopic expression or yeast two-hybrid studies indicate that bacterial flagellins that contain a C-terminal arginine, including *Salmonella*, *Legionella*, and *Pseudomonas,* bind to and activate NAIP5, in contrast to flagellins from *E. coli*, *Burkholderia*, or *Helicobacter*, which contain a C-terminal glutamine, glutamine-glycine, or residue other than arginine (7, 37, 38). Multiple mutations in flagellin that also impact motility are proposed to be necessary to evade NAIP5 recognition (35), making it surprising that a single terminal amino acid would have such an impact on activation of NAIP5/NLRC4. We therefore sought to test the requirement for the C-terminal arginine in NAIP5/NLRC4 inflammasome activation under conditions where flagellin was delivered via a T3SS. We generated an arrayed series of isogenic constructs in which the terminal residue(s) of *S.* Tm or EPEC FliCD0 were mutated to swap glutamine-arginine residues (*SI Appendix*, Fig. S1*C*). *S.* Tm FliCD0 with a glutamine–glycine, which mimics the terminal EPEC FliCD0 sequence, had significantly decreased inflammasome activation relative to WT *S.* Tm FliCD0, as assessed by cell death, IL-1β release, Casp1, and GSDMD cleavage (Fig. 1 *D*–*F*). Removing the terminal arginine of *S.* Tm FliCD0 also significantly reduced cytotoxicity and IL-1β release, and abrogated Casp1 and GSDMD cleavage, indicating that the C-terminal arginine is required for optimal NAIP5/NLRC4 inflammasome activation in response to flagellin (Fig. 1 *D*–*F*). Conversely, replacement of the EPEC FliCD0 C-terminal glutamine–glycine with arginine triggered robust cell death, IL-1β release, as well as GSDMD and Casp1 cleavage at similar levels to *S.* Tm FliCD0 (Fig. 1 *D*–*F*). Intriguingly, glutamine as the penultimate residue at the C terminus abrogated inflammasome activation even when the terminal amino acid itself was arginine, indicating that glutamine at the FliC D0 C terminus acts as a dominant negative to suppress NAIP/NLRC4 inflammasome activation, whereas in the absence of glutamine, arginine following the two

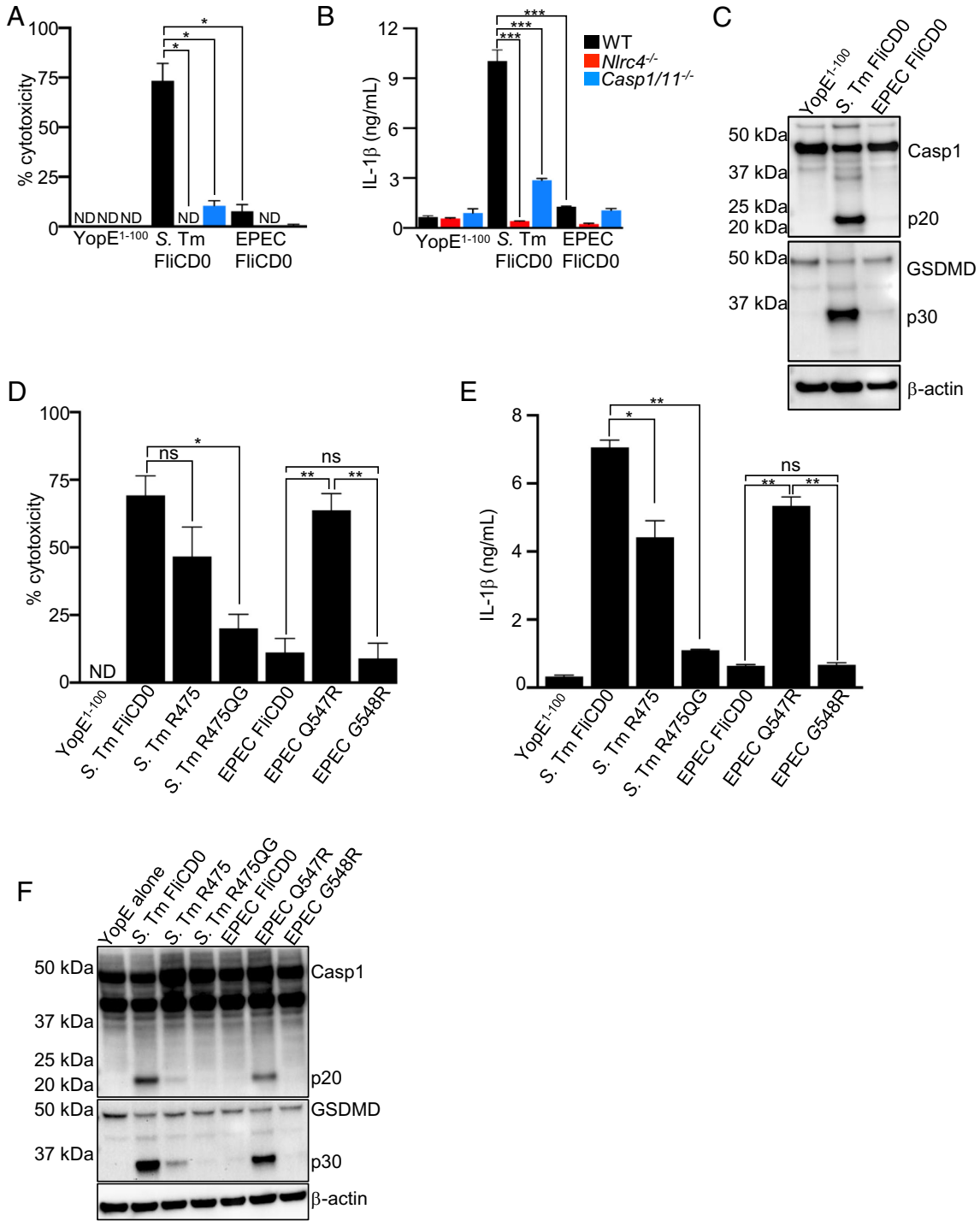

Fig. 1. C-terminal glutamine residues in flagellin disable recognition by the NAIP/NLRC4 inflammasome. (*A* and *B*) WT, *Nlrc4*$^{-/-}$, and *Casp1/11*$^{-/-}$ murine BMDMs were infected with Δ*yopJ Yp* expressing either YopE$^{1\text{-}100}$ or YopE$^{1\text{-}100}$ fused to the C-terminal D0 portion of FliC from *S.* Tm or EPEC for 4 h at an MOI of 20. (*A*) % cytotoxicity was measured via lactate dehydrogenase (LDH) release. (*B*) IL-1β release (ng/mL) was measured by ELISA. (*C*) BMDMs were infected with the indicated strains for 2 h at an MOI of 20. Combined supernatants and cellular lysates were analyzed by immunoblotting for Casp1, GSDMD, and β-actin (loading control). Representative of three independent experiments. (*D* and *E*) WT murine BMDMs were infected with the indicated strains for 4 h at an MOI of 20. (*D*) % cytotoxicity was measured via LDH release. (*E*) IL-1β release (ng/mL) was measured by ELISA. (*F*) BMDMs were infected with the indicated strains for 1 h at an MOI of 20. Combined supernatants and whole cell lysates were analyzed by immunoblotting for Casp1, GSDMD, and β-actin (loading control). Representative of three independent experiments. (*A* and *D*) Data shown are the pooled means ± SEM from three independent experiments. An unpaired *t* test was performed to assess statistical significance. (*B* and *E*) Data shown are the pooled means ± SEM from three independent experiments. Statistical significance was measured by performing an unpaired *t* test. ND = not detected; ns = not significant; **P* < 0.05; ***P* < 0.01; ****P* < 0.001.

conserved leucines is both necessary and sufficient for NAIP/NLRC4 inflammasome activation. Together, these data demonstrate that the *Yp* T3SS delivery system recapitulates the currently known features of NAIP/NLRC4 inflammasome activation by flagellin, and demonstrates a key role for the flagellin C-terminal amino acid in NAIP5 sensing.

TLR Priming Licenses NAIP/NLRC4 Inflammasome Activation by Immunoevasive NAIP Ligands. PRR signaling during bacterial infection up-regulates absent in melanoma (AIM2)-like receptors and NLRP3 to facilitate detection of intracellular PAMPs or DAMPs and is necessary for activation of these inflammasomes (40, 41). While *Naip1* in murine BMDMs is transcriptionally induced by poly-I:C or lipopolysaccharide (LPS) stimulation to enable inflammasome activation by the bacterial T3SS needle (11), *Nlrc4* is not currently known to be transcriptionally induced by PAMP stimulation. However, immune cells at mucosal surfaces are exposed to numerous PAMP-PRR signals from commensal microbes, and infection provides additional exogenous and endogenous inflammatory mediators. We therefore considered the possibility that priming of the NAIP/NLRC4 inflammasome enhances NAIP sensitivity so that evasive ligands like EPEC FliCD0 can be sensed. We therefore primed murine BMDMs with synthetic triacylated lipopeptide (Pam3CSK4 or Pam3), diacylated lipopeptide (Pam2CSK4 or Pam2), LPS, or the inflammatory cytokine interferon-γ (IFN-γ). Intriguingly, BMDMs primed with the TLR2 ligands Pam3, Pam2, or TLR4 ligand LPS, but not IFN-γ, exhibited increased cell death and IL-1β release in response to EPEC FliCD0 (*SI Appendix*, Fig. *S2 A* and *B*). Cell death and IL-1β release in Pam3-primed cells were dependent on NLRC4, Casp1, and NAIP5, indicating that priming enhances the ability of NAIP5 to detect immunoevasive flagellins, rather than enabling NAIP6 to compensate for NAIP5 (Fig. 2 *A* and *B*). This increased cytotoxicity and IL-1β release in Pam3-primed cells in response to EPEC FliCD0 correlated with elevated GSDMD cleavage and Casp1 cleavage (Fig. 2*C* and *SI Appendix*, Fig. S2*C*). Notably, Pam3 priming also induced elevated cytotoxicity and IL-1β release in response to mutant versions of *S*. Tm FliCD0 that contain C-terminal glutamine, indicating that TLR priming overcomes the inhibitory effect of glutamine on NAIP5/NLRC4 activation (*SI Appendix*, Fig. S3 *A* and *B*). In Pam3-primed cells, control infection with *Yp* expressing $YopE^{1\text{-}100}$ alone induced significant levels of IL-1β release with minimal levels of cytotoxicity or processing of Casp1 or GSDMD (Fig. 2 *A*–*C*). However, this release of IL-1β in response to YopE alone was independent of NAIP5, indicating that this response is distinct from the NAIP/NLRC4-dependent pathway induced by flagellin, but is NLRC4 and Casp1/11-dependent, suggesting that it was likely due to priming-induced responses to *Yersinia* T3SS needle or rod proteins (50) (Fig. 2*B*).

The NLRP3 inflammasome requires priming (termed "signal 1") to undergo inflammasome activation (40, 51) and can synergize with NLRC4 for maximal responses to *S*. Tm and other bacterial pathogens (16, 52, 53). Notably, $Nlrp3^{-/-}$ BMDMs were unaffected in their ability to undergo priming-induced cytotoxicity or IL-1β release in response to cytosolic delivery of EPEC FliCD0 (*SI Appendix*, Fig. S3 *C* and *D*), indicating that NLRP3 does not contribute to TLR-induced priming of NAIP/NLRC4 responses to immunoevasive flagellin. This was also the case for BMDMs lacking the inflammasome adaptor protein ASC, indicating that TLR-induced activation of the NAIP/NLRC4 inflammasome by evasive EPEC FliCD0 requires an intact NAIP-NLRC4-Casp1 signaling axis but not NLRP3 or ASC to drive pyroptosis (*SI Appendix*, Fig. S3 *E* and *F*).

In addition to NAIP5/NLRC4 inflammasome evasion by changes in the C-terminal FliCD0 domain, a number of pathogens produce T3SS needle and inner rod proteins that also evade NAIP/NLRC4 detection in murine macrophages to enable intracellular replication (10). This includes the SsaI inner rod subunit of the SPI-2 T3SS in *S*. Tm and the SPI-2 T3SS needle protein SsaG, though human NAIP is capable of detecting SsaG but not SsaI (16). Furthermore, the EPEC needle, EscF (34, 54), is also not sensed by the NAIP/NLRC4 inflammasome (8), raising the question of whether TLR priming of the NAIP/NLRC4 inflammasome enhances recognition of other classes of immunoevasive NAIP ligands in addition to flagellin. We therefore evaluated the cytotoxicity of Pam3-primed and unprimed BMDMs infected with *Yp* expressing YopE fused to *S*. Tm SsaG or SsaI, as well as EPEC EscF. As expected, unprimed BMDMs did not respond to these ligands (Fig. 2 *D* and *E*). However, Pam3-primed BMDMs exhibited significantly increased cell death and IL-1β release in response to SsaG, SsaI, and EscF, suggesting that murine macrophages are able to detect immunoevasive NAIP ligands when stimulated through TLR2 (Fig. 2 *D* and *E*). Similar to SPI-2 ligands, priming of BMDMs led to increased cell death and IL-1β release in response to cytosolic delivery of EscF (Fig. 2 *D* and *E*). The increase in cell death and IL-1β release in primed cells in response to T3SS components correlated with an increase in Casp1 and GSDMD cleavage (Fig. 2*F*). Altogether, our data reveal that TLR priming licenses the NAIP/NLRC4 inflammasome to detect normally evasive ligands.

TLR Priming Up-Regulates NLRC4 Expression via p38 MAPK Signaling. Pam3 and Pam2 are ligands for TLR2, which requires the adaptor MyD88 to transduce responses (55). Consistently, increased cell death in response to EPEC FliCD0 required MyD88 in BMDMs primed with Pam3 or Pam2, but not with LPS, suggesting that LPS-induced TRIF signaling can also induce this priming (*SI Appendix*, Fig. *S2 A* and *B*). We next considered the possibility that TLR priming might impact the expression of *Naip* or *Nlrc4* genes. While *Naip1* is induced by poly(I:C), and steady-state levels of *Nlrc4* and *Naips* require the transcription factor IRF8 and epigenetic reader BRD4 (11, 42, 43), it is not thought that other components of the NAIP/NLRC4 inflammasome are under inducible transcriptional control. Intriguingly, while we observed no increase in messenger RNA (mRNA) expression of *Naip1* or *2*, and a small decrease in expression of *Naip5* and *6*, *Nlrc4* levels exhibited a significant increase in response to Pam3CSK4 (Fig. 3*A* and *SI Appendix*, Fig. S4*A*). Furthermore, Pam3 signaling induced NLRC4 protein expression in a dose-dependent manner (Fig. 3*B*). Interestingly, we observed a trend toward increased transcript and protein levels at 8 h postpriming, while the highest levels of *Nlrc4* transcript and NLRC4 protein occurred 16 h postpriming (*SI Appendix*, Fig. *S4 B* and *C*). Notably, stimulation with either Pam2 or LPS, but not IFN-γ, also increased *Nlrc4* mRNA abundance and protein levels after 16 h postpriming (*SI Appendix*, Fig. *S4 B* and *C*). These data indicate that TLR2/4 signaling, but not IFN-γ signaling, regulates NLRC4 expression in BMDMs.

We next sought to determine the basis for transcriptional induction of *Nlrc4* in response to TLR priming. TLR signaling leads to activation of both nuclear factor kappa B and the MAPK signaling cascades to promote inflammatory gene transcription. Recently, the MAPK p38 has been implicated in controlling NLRP1 inflammasome activation in response to cellular stress (56, 57). Furthermore, as BRD4 has been implicated in IRF8-mediated developmental transcription of *Nlrc4* (42) and p38 can activate BRD4 activity in other cell types (58), we considered that p38 MAPK may contribute to TLR2-based priming of the NAIP/NLRC4 inflammasome to immunoevasive NAIP ligands. Notably, inhibition of p38 MAPK activity prevented Pam3-induced upregulation of *Nlrc4* transcript and protein (Fig. 3 *C* and *D*) as well as a known TLR-induced transcript, *Il6* (*SI Appendix*, Fig. S5*A*), but did not impact basal NLRC4 expression in the absence of priming (*SI Appendix*, Fig. S5 *B* and *C*). Critically, p38 MAPK inhibition also abrogated Pam3-induced cytotoxicity in response to EPEC FliCD0, and

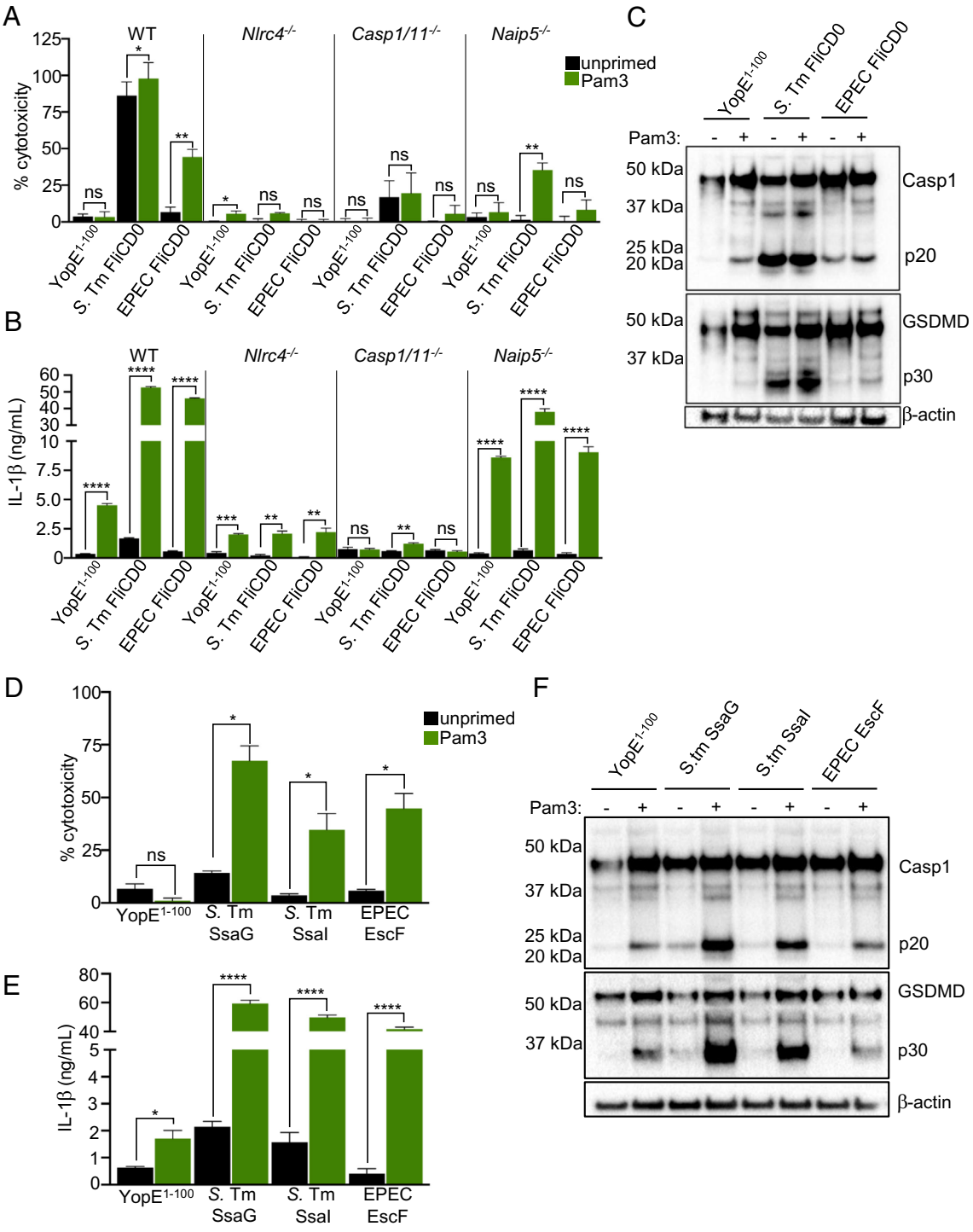

Fig. 2. TLR priming licenses NAIP/NLRC4 inflammasome activation by immunoevasive NAIP ligands. (*A* and *B*) WT, *Nlrc4*$^{-/-}$, *Casp1/11*$^{-/-}$, and *Naip5*$^{-/-}$murine unprimed BMDMs or primed with 0.5 μg/mL Pam3CSK4 (Pam3) for 16 h were infected with the indicated strains for 4 h at an MOI of 20. (*A*) Cell death (% cytotoxicity) was measured via LDH release. (*B*) IL-1β release (ng/mL) was measured by the ELISA. (*C*) BMDMs were infected with the indicated strains for 4 h at an MOI of 20, and TCA-precipitated supernatants and whole cell lysates were collected and combined. Samples were analyzed by immunoblot for Casp1, GSDMD, and β-actin (loading control). Image representative of three independent experiments. (*D* and *E*) WT murine unprimed BMDMs or primed with 0.5 μg/mL Pam3CSK4 for 16 h were infected with the indicated strains for 2 h at an MOI of 20. (*D*) % cytotoxicity was measured via LDH release. (*E*) IL-1β release (ng/mL) was measured by the ELISA. (*F*) BMDMs were infected with the indicated strains for 4 h at an MOI of 20. Combined supernatants and whole cell lysates were analyzed by immunoblotting for Casp1, GSDMD, and β-actin (loading control). Image representative of three independent experiments. (*A* and *D*) Data shown are pooled means ± SEM from three independent experiments. A paired *t* test was performed to assess statistical significance. (*B* and *E*) Data shown are representative of three independent experiments and are the combined means ± SEM. Statistical significance was measured by performing an unpaired *t* test. ns = not significant; *$P < 0.05$; **$P < 0.01$; *** $P < 0.001$; ****$P < 0.001$.

reduced the response to *S.* Tm FliC D0 to that of unprimed cells (Fig. 3*E*). These data indicate that TLR2 stimulation up-regulates NLRC4 via a p38 MAPK-dependent pathway and suggest that increased NLRC4 levels enable activation of the murine NAIP/NLRC4 inflammasome in response to suboptimal or immunoevasive ligands. To test whether increasing the expression of NLRC4 is sufficient to enable responses to immunoevasive flagellins, we ectopically expressed murine NLRC4 in immortalized

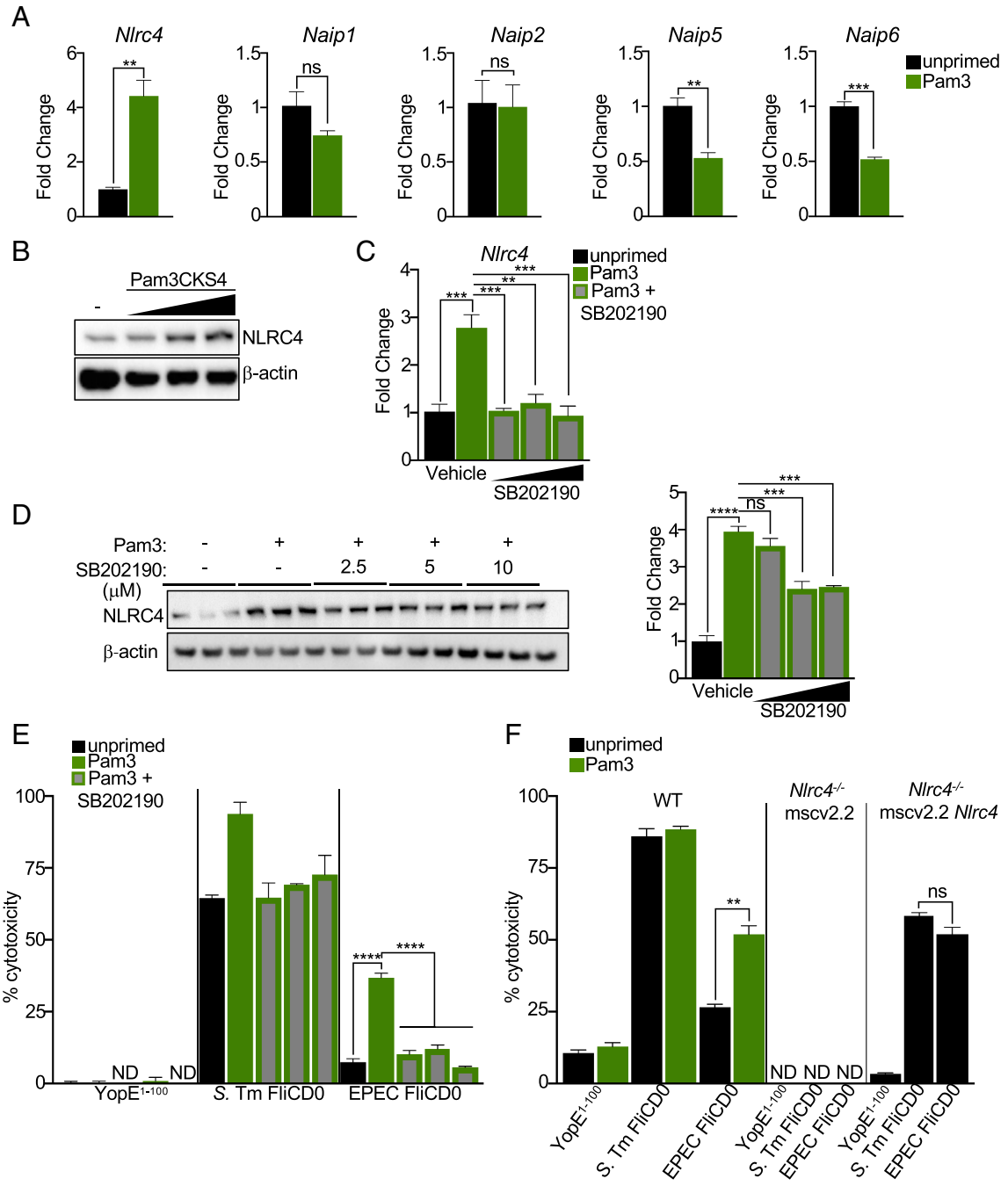

Fig. 3. TLR priming up-regulates NLRC4 expression via p38 MAPK signaling. (*A* and *B*) WT murine BMDMs were unprimed or primed for 16 h with (*A*) 0.5 μg/mL Pam3CSK4 or (*B*) 0.25 μg/mL, 0.5 μg/mL, or 1 μg/mL Pam3CSK4. (*A*) *Nlrc4, Naip1, Naip2, Naip5,* and *Naip6* transcripts were assessed via qRT-PCR, and fold change was assessed relative to unstimulated BMDMs. (*B*) NLRC4 protein levels were assessed via immunoblot. Data are representative of three independent experiments. (*C*–*E*) WT murine BMDMs were unprimed or primed with 0.5 μg/mL Pam3CSK4. One hour prior to priming, the BMDMs were treated with 2.5 μM, 5 μM, or 10 μM p38 MAPK inhibitor SB202190 or Dimethyl sulfoxide (DMSO) vehicle control. (*C*) *Nlrc4* transcript levels relative to *Gapdh* were assessed via qRT-PCR. Fold change was determined relative to unstimulated control. (*D*) NLRC4 protein levels were analyzed via immunoblot. NLRC4 protein intensity was quantified relative to loading controls, and average fold change ± SEM in NLRC4 protein levels was assessed relative to unstimulated DMSO-treated cells. Data are representative of three independent experiments. (*E*) % cytotoxicity was measured via LDH release 2 h postinfection with the indicated strains at an MOI of 20. (*F*) Immortalized ER-Hoxb8 *Nlrc4*$^{-/-}$ murine macrophages were transduced with the retroviral mscv2.2 vector alone (mscv2.2) or mscv2.2 overexpressing *Nlrc4* (mscv2.2 *Nlrc4*). WT macrophages, *Nlrc4*$^{-/-}$ macrophages transduced with mscv2.2, or *Nlrc4*$^{-/-}$ macrophages transduced with mscv2.2 *Nlrc4* were infected with indicated *Yp* strains expressing YopE$^{1\text{-}100}$, *S.* Tm FliCD0, and EPEC FliCD0 for 2 h at an MOI of 20. % cytotoxicity was measured via LDH release. Only WT ER-Hoxb8 cells were primed for 16 h with Pam3CSK4. (*A*, *C*, *E*, and *F*) Data shown are representative of three experiments. Means ± SEM are shown (n = 3) and statistical significance was measured by performing an unpaired *t* test (*A* and *F*) or 1-way ANOVA (*C*–*E*). ND = not detected; ns = not significant; ***P* < 0.01; ****P* < 0.001; *****P* < 0.0001

Nlrc4$^{-/-}$ BMDMs (*SI Appendix*, Fig. S5*D*). Intriguingly, whereas WT iBMDMs exhibited Pam3 priming-dependent cytotoxicity in response to cytosolic delivery of EPEC FliCD0, iBMDMs overexpressing NLRC4 did not require priming in order to respond to EPEC FliCD0 (Fig. 3*F*), demonstrating that increased NLRC4 expression is sufficient to enable NAIP/NLRC4 inflammasome detection of immunoevasive flagellins. Moreover, inhibition of p38 did not abrogate cytotoxicity in response to EPEC FliCD0 in iBMDMs overexpressing NLRC4 (*SI Appendix*, Fig. S5*E*), demonstrating that increasing expression of NLRC4 bypasses the requirement for p38-dependent signaling in enhancing responses to immunoevasive flagellin.

NLRC4 phosphorylation at S533 residue has been implicated in enhancing NLRC4 activity (59, 60). To investigate whether phosphorylation of NLRC4 at S533 was responsible for priming-induced NLRC4 activation, we quantified cytotoxicity in response to EPEC FliCD0 in primed and unprimed BMDMs from NLRC4^{S533A} mice, which are defective in NLRC4 phosphorylation (60). Consistent with previous observations, mutation of S533 had a modest effect on NLRC4-dependent cell death in response to *Salmonella* flagellin in unprimed cells (*SI Appendix*, Fig. S5*F*). However, Pam3 priming still elicited increased cell death in response to EPEC FliCD0 in NLRC4^{S533A} BMDMs (*SI Appendix*, Fig. S5*F*). Therefore, while NLRC4 phosphorylation contributes to maximal NLRC4 activity, these data indicate that it is not required for enhanced NAIP/NLRC4 inflammasome activation by immunoevasive flagellin following Pam3 priming.

The Human NAIP/NLRC4 Inflammasome Does Not Respond to TLR Priming to Detect Evasive Flagellin. In contrast to mice, humans express a single NAIP that broadly detects bacterial flagellin and T3SS structural components (14, 15, 17). Human NAIP is capable of detecting the SPI-2 needle protein SsaG from *Salmonella* to restrict intracellular bacterial replication, suggesting that the broader specificity of the single human NAIP could potentially enable detection of a wider range of ligands (16). As expected, human THP-1 monocyte-derived macrophages exhibited robust responses to *S.* Tm FliCD0 delivered by the *Yp* T3SS that was dependent on NLRC4 and NAIP (Fig. 4*A*). Surprisingly however, THP-1 monocyte-derived macrophages did not respond to the EPEC FliCD0 domain, despite being basally stimulated with Pam3 (Fig. 4*A*). Notably, and in marked contrast to their murine counterparts, THP-1 monocyte-derived macrophages exhibited reduced levels of *NLRC4* transcript when treated with Pam3, Pam2, or LPS, indicating that human and murine *NLRC4* genes exhibit distinct transcriptional responses to TLR stimulation (Fig. 4*B*). Human *NAIP* transcript levels were similarly reduced in response to TLR stimuli, and contrasted with the control gene *IL6*, which was dramatically up-regulated by all stimuli (Fig. 4*B*). Moreover, in contrast to murine NLRC4, human NLRC4 protein levels were unaltered in response to Pam3 stimulation, suggesting that the human NAIP/NLRC4 inflammasome does not undergo priming in response to TLR ligands (Fig. 4*C*). This is not due to a lack of p38 activation in human cells following TLR priming, as p38 phosphorylation was robustly activated in both human and murine macrophages following Pam3 stimulation (*SI Appendix*, Fig. S5*G*) Importantly, primary human monocyte-derived macrophages (hMDMs) also failed to detect the EPEC FliCD0 domain even after Pam3 priming, as levels of IL-1β released in response to EPEC FliCD0 were identical to the YopE1-100 alone, in contrast to *S.* Tm FliCD0 (Fig. 4*D*). Similarly to murine NLRC4, expression of human NLRC4 in immortalized murine BMDMs resulted in priming-independent responses to cytosolic delivery of EPEC FliCD0 (Fig. 4*E*). Critically, overexpression of human NLRC4 in human THP-1 monocyte-derived macrophages was also sufficient to enable human cells to detect the EPEC FliCD0 domain (Fig. 4*F*). Together, these data indicate that in contrast to murine macrophages, human NLRC4 does not undergo TLR-induced priming and that expression levels of NLRC4 also modulate the ability of the human NAIP/NLRC4 inflammasome to undergo activation in response to evasive ligands.

TLR Priming Overcomes Evasion of the NAIP/NLRC4 Inflammasome during Infection. We next asked whether TLR priming enables the NAIP/NLRC4 inflammasome to respond to bacteria expressing full-length flagellin containing terminal glutamine–glycine residues in the context of the endogenous flagellar apparatus and T3SS during infection. We generated a *S.* Tm strain in which the terminal arginine at the endogenous FliC locus was replaced with glutamine-glycine. To ensure that NAIP/NLRC4 inflammasome responses to this mutant flagellin were not confounded by FljB, the *Salmonella* alternate phase flagellin, we performed these studies in a *fljB* mutant background. As expected, given normal motility of EPEC as well as other bacteria with flagellins that contain terminal glutamine–glycine rather than arginine residues, *S.* Tm expressing FliC^{R475QG} exhibited motility that was indistinguishable from wild-type bacteria (*SI Appendix*, Fig. S6*A*). Critically, *S.* Tm carrying a mutation of the FliC C-terminal arginine to glutamine–glycine induced significantly lower cytotoxicity during infection of WT murine BMDMs, which was restored by Pam3 priming (Fig. 5*A*). Furthermore, consistent with our findings that human macrophages are deficient in their ability to respond to immunoevasive flagellins regardless of priming, THP-1 cells primed with Pam3 had low levels of IL-1β release in response to *S.* Tm expressing FliC^{R475QG} that was comparable to that of unprimed WT or NAIP-deficient cells (Fig. 5*B*).

Given that TLR2/4 signaling enables the murine NAIP/NLRC4 inflammasome to sense evasive ligands in vitro, we wondered whether similar priming of the NAIP/NLRC4 inflammasome might occur in response to inflammatory stimuli in vivo. We therefore primed mice in vivo by intraperitoneal injection of heat-killed *S.* Tm and assayed the response of peritoneal cells isolated from primed mice to immunoevasive flagellin. Indeed, peritoneal cells isolated from primed mice exhibited significantly increased levels of cytotoxicity and IL-1β release in response to EPEC FliCD0 (Fig. 5 *C* and *D*). Furthermore, isolated naïve peritoneal macrophages that were primed in vitro also exhibited increased IL-1β release and had elevated levels of NLRC4 in response to EPEC FliC D0 (*SI Appendix*, Fig. S6*B*). Finally, to test how flagellar evasion of NAIP sensing might impact immune responses during infection in vivo, we infected C57BL6/J (WT) mice with isogenic *S.* Tm strains expressing either WT native FliC or FliCR475QG, and assayed serum IL-18 levels 48 h postinfection. Critically, consistent with our in vitro observations, *Salmonella* expressing flagellin that is poorly recognized by NAIP5 induced lower levels of serum IL-18 compared with *Salmonella* expressing native immunostimulatory *Salmonella* FliC, despite having similar splenic bacterial burdens (Fig. 5*E* and *SI Appendix*, Fig. S6*C*). Altogether, these data indicate that the response to bacterial infection in vivo is reduced by alteration of amino acids that regulate NAIP sensing, and that in vivo priming of the murine NAIP/NLRC4 inflammasome can facilitate cytosolic detection of immunoevasive flagellin.

Discussion

We report here a T3SS-based system for delivery of T3SS and flagellin-derived NAIP ligands into the host cell cytosol. Our studies reveal that TLR- and p38 MAPK-mediated upregulation of murine NLRC4 expression enables the NAIP/NLRC4 inflammasome to respond to ligands that evade NAIP detection. Interestingly, human macrophages were both basally insensitive to immunoevasive flagellin and were insensitive to TLR-induced priming, which correlated with their inability to respond to immunoevasive flagellin delivered through the T3SS. Notably, ectopic expression of murine or human NLRC4 in both murine and human macrophages, however, conferred enhanced inflammasome responses against immunoevasive flagellin. Our findings reveal a mechanism for tuning the sensitivity of the NAIP/NLRC4 inflammasome to suboptimal ligands by controlling expression of its adaptor, NLRC4.

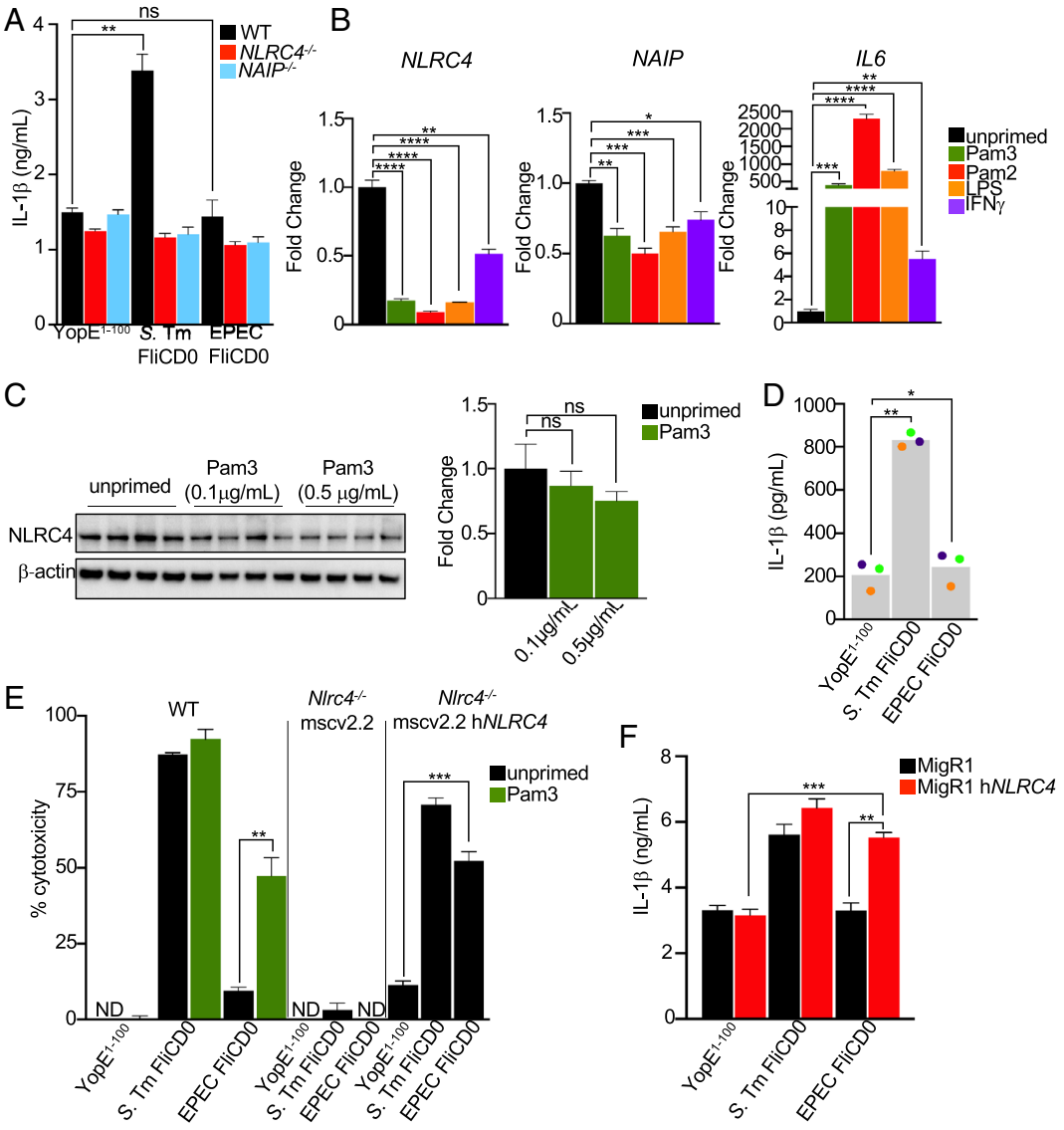

Fig. 4. The human NAIP/NLRC4 inflammasome does not respond to TLR priming to detect evasive flagellin. (*A*) WT, *Nlrc4*$^{-/-}$, or *Naip*$^{-/-}$ THP-1 macrophages were primed with 0.1 μg/mL Pam3CSK4 for 16 h and infected with WT *Yp* expressing either YopE$^{1\text{-}100}$, *S.* Tm FliCD0, or EPEC FliCD0 at an MOI of 60 for 6 h. IL-1β release (ng/mL) was measured by the ELISA. (*B* and *C*) WT THP-1 macrophages were primed with 0.1 μg/mL (*B* and *C*) or 0.5 μg/mL (*C*) Pam3CSK4, 0.05 μg/mL Pam2CSK4, 100 ng/mL LPS, or 100 ng recombinant human IFN-γ for 16 h. (*B*) *Nlrc4, Naip,* and *Il6* transcript levels relative to *Hprt* were assessed via qRT-PCR. Fold change in transcript levels was analyzed relative to unstimulated control. (*C*) NLRC4 protein levels were analyzed via immunoblot. NLRC4 protein intensity was quantified relative to loading controls, and fold change in NLRC4 protein levels was assessed relative to unstimulated cells. Data are representative of three independent experiments. (*D*) Primary hMDMs from three healthy human donors were primed with 0.1 μg/mL Pam3CSK4 for 16 h and infected with indicated strains at an MOI of 60 for 6 h. IL-1β release (pg/mL) was measured by the ELISA. Each dot represents the mean of each donor derived from triplicate wells. Bars depict the mean of three donors. (*E*) Immortalized ER-Hoxb8 *Nlrc4*$^{-/-}$ murine macrophages were transduced with the retroviral mscv2.2 vector alone or mscv2.2 overexpressing human *NLRC4* (mscv2.2h*NLRC4*). WT, *Nlrc4*$^{-/-}$mscv2.2, or *Nlrc4*$^{-/-}$ mscv2.2h*NLRC4* macrophages were infected with indicated strains for 2 h at an MOI of 20. % cytotoxicity was measured via LDH release. Only WT Hoxb8 cells were primed for 16 h with Pam3CSK4. (*F*) THP-1 hMDMs transduced with the MigR1 retroviral vector alone or overexpressing h*NLRC4* were primed with 0.1 μg/mL Pam3CSK4 for 16 h and infected with WT *Yp* expressing either YopE$^{1\text{-}100}$, *S.* Tm FliCD0, or EPEC FliCD0 at an MOI of 60 for 6 h. IL-1β release (ng/mL) was measured by the ELISA. (*A*–*F*) Data shown are representative of three independent experiments. Means ± SEM are shown (n = 3) and statistical significance was measured by performing an unpaired *t* test (*A*, *C*, *E*, and *F*) or paired *t* test (*D*) or 1-way ANOVA (*B*). ND = not detected; ns = not significant; *P < 0.05; **P < 0.01; ***P < 0.001; ****P < 0.0001.

In the absence of TLR priming, in addition to the conserved C-terminal leucine residues, which are required for NAIP5-dependent sensing of flagellin (35, 36), a C-terminal arginine is also required for NAIP5/NLRC4-dependent inflammasome activation via T3SS-delivered FliC (37, 38). Intriguingly, a large number of human-specific bacterial pathogens, including EPEC, *Shigella*, *Helicobacter*, *Clostridioides difficile*, among others, encode flagellin sequences that contain C-terminal glutamine, glutamine-glycine, or other nonarginine residues, that empirically do not activate or would be predicted to evade the NAIP5/NLRC4 inflammasome. A number of these flagellins have been reported to not be bound by NAIP5, leading to a model where NAIP5 binding is the determining feature of NAIP5/NLRC4 inflammasome activation (7, 37, 38).

Bacterial flagellins and T3SS components that are poor stimulators of the NAIP/NLRC4 inflammasome have been thought to not bind their cognate NAIPs, and whether a mechanism might exist to enable the host to overcome this type of evasion strategy by flagellins, or other immunoevasive NAIP ligands, has not yet been described. Interestingly, *Shigella* is not known to express flagella (61), although it encodes a flagellin gene that contains a terminal -QG, and which initial reports indicated does not bind NAIP5 in yeast two-hybrid based studies (7). Nevertheless, ectopic expression of *Shigella* flagellin in murine macrophages leads to NLRC4-dependent lethality (36).

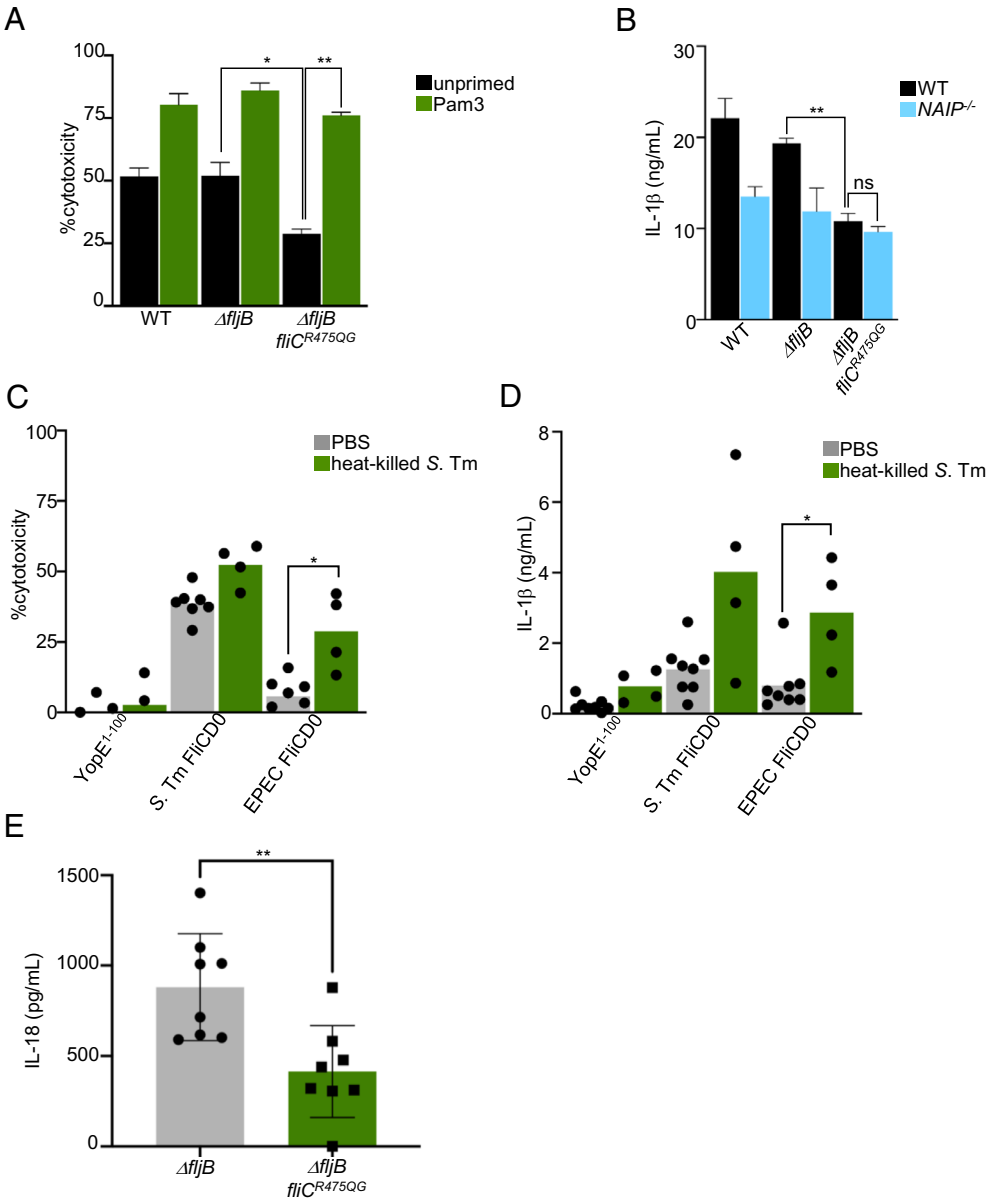

Fig. 5. TLR priming overcomes evasion of the NAIP/NLRC4 inflammasome during infection. (*A*) WT murine unprimed BMDMs or primed with 0.5 μg/mL Pam3CSK4 for 16 h were infected with WT, Δ*fljB*, or Δ*fljB fliC*^{R475QG} *S.* Tm for 1 h at an MOI of 20. % cytotoxicity was measured via LDH release. (*B*) WT or *Naip*$^{-/-}$ THP-1 human macrophages were primed with 0.1 μg/mL Pam3CSK4 for 16 h and infected with WT, Δ*fljB,* or Δ*fljB fliC*^{R475QG} *S.* Tm for 6 h at an MOI of 60. IL-1β release (pg/mL) was measured by the ELISA. (*C* and *D*) Total peritoneal exudate cells were harvested from WT C57Bl/6J mice intraperitoneally injected with heat-killed *S.* Tm (green bars) or PBS (gray bars) and then infected with the indicated *Yp* strains for 2 h at an MOI of 20. (*C*) % cytotoxicity was measured via LDH release. (*D*) IL-1β release (pg/mL) was measured by the ELISA. Each dot represents the mean of one mouse derived from triplicate wells. n = 7 for PBS-treated mice and n = 4 for heat-killed *S.* Tm-treated mice. Bars represent the means of all mice and statistical analyses were performed using a Mann–Whitney test. (*E*) WT C57Bl/6J mice were intraperitoneally infected with 500 CFUs of either Δ*fljB* or Δ*fljB fliC*^{R475QG} *S.* Tm for 48 h. Serum IL-18 levels (pg/mL) were measured by the ELISA. Data shown are combined ± SEM from two independent experiments. An unpaired *t* test was performed to assess statistical significance. (*A*) Data shown are means ± SEM pooled from three independent experiments, and a paired *t* test was performed to assess statistical significance. (*B*) Data shown are representative of one out of at least three independent experiments. Means ± SEM are shown (n = 3), and statistical significance was measured by performing an unpaired *t* test. ns = not significant; **P* < 0.05; ***P* < 0.01.

These data suggest that the innate immune system can detect evasive flagellins and other NAIP ligands under some conditions. Our findings demonstrate that TLR-dependent upregulation of NLRC4 expression enables activation of the murine NAIP5/NLRC4 inflammasome in response to evasive flagellins. We find that the main determinant of NAIP5 evasion by flagellin is the presence of a C-terminal glutamine, which can act in a dominant manner in-*cis* to suppress flagellin detection by NAIP5, and that TLR priming overcomes this evasion. TLR priming of the murine NAIP/NLRC4 inflammasome thus represents a potential adaptation that allows the host to overcome microbial immune evasion in the ongoing evolutionary arms race between pathogens and their hosts.

While the NLRP3 and AIM2 inflammasomes are transcriptionally up-regulated in response to inflammatory signals, other than NAIP1, the NAIP/NLRC4 inflammasome is generally not considered to be subject to transcriptional priming (11, 40, 41). NAIP5/NLRC4 inflammasome assembly is initiated by a single NAIP5 subunit that, upon binding flagellin, undergoes a conformational change that recruits and induces a conformational change in the first NLRC4 subunit, which in turn uncovers a binding surface to recruit and induce polymerization of subsequent NLRC4 subunits (19, 21, 35, 39, 62). NLRC4 is therefore not thought to be limiting for inflammasome activation. Indeed, our data indicate that TLR priming or ectopic expression of NLRC4 has limited impact on

inflammasome responses to activating flagellin from *S*. Tm, in contrast to evasive flagellin from EPEC. Conversely, blockade of p38 MAPK signaling, which significantly blunted both the Pam3-induced upregulation of *Nlrc4* and the NAIP/NLRC4 response to immunoevasive flagellin, also had limited impact on the response to *S*. Tm FliCD0. Collectively, these findings indicate that expression levels of NLRC4 tune the ability of murine macrophages to detect suboptimal NAIP ligands.

Because EPEC flagellin and other poorly activating/evasive ligands were not thought to be bound by their cognate NAIP, they were not predicted to be able to nucleate NLRC4 polymerization. We propose that the low-affinity between NAIP and evasive ligands results in an unstable complex with a short half-life that does not provide enough time for nucleation and polymerization of NLRC4 (*SI Appendix*, Fig. S7). However, our findings suggest that cells with elevated NLRC4 expression will exhibit increased NAIP/NLRC4 avidity, such that a low-affinity ligand–NAIP complex has an increased likelihood to be stabilized by recruitment of the initial NLRC4 subunit, thereby enabling subsequent NLRC4 polymerization and inflammasome activation to take place (*SI Appendix*, Fig. S7). Our findings imply that in addition to NAIP–ligand binding being a key rate-limiting step in NAIP/NLRC4 inflammasome activation, NAIP/NLRC4 avidity may help to set the threshold for inflammasome activation and that this threshold is tuned by TLR-induced regulation of NLRC4 expression. Structural approaches, such as cryogenic electron microscopy, may help visualize the formation of the NAIP-NLRC4 inflammasome in response to immunoevasive flagellin with and without TLR priming, further testing this hypothesis.

Humans express a single NAIP that broadly detects flagellin, T3SS needle, and rod proteins (14, 15, 17). While this promiscuity allows for broader sensing of multiple ligands, human NAIP also does not respond to evasive flagellin or T3SS inner rod proteins. Surprisingly, TLR priming did not induce a response to immunoevasive flagellins in human macrophages, suggesting either that the NAIP/NLRC4 system in humans cannot be primed to sense immunoevasive ligands, or that it may be primed by distinct stimuli. Notably, TLR priming did not significantly affect *NLRC4* expression in human macrophages, in contrast to our observations in mouse macrophages, suggesting that the NAIP/NLRC4 inflammasome is subject to distinct regulatory controls in humans and mice. Given the presence of poorly activating terminal amino acids in a large number of human-specific pathogens (7, 37, 38), and the recent findings that NLRC4 serves as an important barrier in mice to colonization by *Shigella* (32, 33), it is tempting to speculate that species-specific transcriptional regulation of the NAIP/NLRC4 inflammasome contributes to the shaping of the repertoire of commensal and pathogenic microbes that colonize specific host niches.

Altogether, our findings uncover a role for TLR stimulation in transcriptionally regulating the NAIP/NLRC4 inflammasome and licensing detection of immunoevasive NAIP ligands in murine cells. These findings shed light on species-specific control of NAIP/NLRC4 inflammasome responses and have implications for the differential ability of pathogens to evade the NAIP/NLRC4 inflammasome in mice and humans.

Ethics Statement. All animal studies were performed in compliance with the federal regulations set forth in the Animal Welfare Act, the recommendations in the Guide for the Care and Use of Laboratory Animals of the NIH, and the guidelines of the University of Pennsylvania Institutional Animal Use and Care Committee. All protocols used in this study were approved by the Institutional Animal Care and Use Committee at the University of Pennsylvania, (Animal Welfare Assurance Number D16-00045/A3079-01, Protocol #804523). All experiments on primary hMDMs were performed in compliance with the requirements of the US Department of Health and Human Services and the principles expressed in the Declaration of Helsinki. hMDMs were derived from samples obtained from the University of Pennsylvania Human Immunology Core, and they are considered to be a secondary use of deidentified human specimens and are exempt via Title 55 Part 46, Subpart A of 46.101 (b) of the Code of Federal Regulations.

Materials and Methods

Bacterial Strains and Growth Conditions. A complete list of strains is found in *SI Appendix*, Table S1. All *Yp* strains were grown in 2× yeast extract tryptone (YT) broth at 28 °C in a shaking incubator at 250 rpm. All *S*. Tm, EPEC, and *E. coli* strains were grown in Luria–Bertani Broth (LB) Miller's formulation at 37 °C in a shaking incubator at 250 rpm. When solid medium was required, LB plates containing 1.5% agar supplemented with the appropriate antibiotics were used to incubate either *Yp* for 48 h or *S*. Tm strains overnight (O/N) at 28 °C or 37 °C, respectively.

***Yersinia*-Mediated Delivery of NAIP Ligands.** Primers for cloning of NAIP ligands for *Yersinia*-mediated delivery are described in *SI Appendix*, Table S2. Briefly, the coding region for the terminal 35 amino acids in the D0 domain of respective genes was inserted downstream of the *yopE* promoter sequence and the coding sequence of the first 100 amino acids of *yopE* from *Yp* 32777. Constructs were ligated into expression vector pACYC184 using BamHI and SalI restriction sites. Point mutations of the pACYC184 YopE- *S*.Tm or EPEC FliCD0 constructs were generated with the Q5 site-directed mutagenesis kit (New England Biolabs) following manufacturer recommendations. All constructs were validated by Sanger sequencing.

Isolation and Growth of BMDMs. BMDMs were isolated and differentiated as previously described (49). Briefly, bone marrow cells isolated from 6 to 10-wk-old mice were grown at 37 °C, 5% CO_2 in 30% macrophage media (30% L929 fibroblast supernatant, complete Dulbecco's Modified Eagle Medium (DMEM)). BMDMs were harvested in cold PBS on day 7 and replated in 10% macrophage media onto tissue culture-treated plates prior to subsequent infection. BMDMs were primed with 0.5 μg/mL Pam3CSK4 (Invivogen), 0.05 μg/mL Pam2CSK4 (Invivogen), 100 ng/mL LPS (Sigma), and 100 ng IFN-γ (BioLegend) as indicated in the figure legends for 16 to 20 h prior to bacterial infection or harvesting for immunoblot or RNA isolation.

THP-1 and hMDM Growth Conditions. THP-1 cells (TIB-202; American Type Culture Collection) were maintained in THP-1 growth medium (RPM1 with 10% (vol/vol) heat-inactivated fetal bovine serum (FBS) + 0.05 nM β-mercaptoethanol + 100 IU/mL penicillin + 100 μg/mL streptomycin) and incubated at 37 °C, 5% CO_2. Human monocytes purified from deidentified healthy human donors were obtained from the University of Pennsylvania Human Immunology Core. To derive the human monocytes into hMDMs, the cells were cultured in RPMI supplemented with 10% (vol/vol) heat-inactivated FBS + 2 mM L-glutamine + 100 IU/mL penicillin + 100 μg/mL streptomycin + 50 ng/mL recombinant human M-CSF (Gemini Bio-Products) for 6 d at 37 °C, 5% CO_2. *Nlrc4*$^{-/-}$ and *Naip*$^{-/-}$ THP-1 cells were previously described (16).

Infection of Macrophages. *Yp* strains were induced to up-regulate expression of the T3SS and associated effectors by taking 100 μL of stationary phase overnight cultures and adding to 3 mL 2× YT media containing 20 mM sodium oxalate (Sigma) and 20 mM MgCl (Sigma), followed by shaking at 28 °C for 1 h and shifting to a 37 °C shaking incubator for 2 additional hours. To induce SPI-1 expression in *S*. Tm, 100 μL of overnight cultures were added to 3 mL LB containing 300 mM NaCl and grown at 37 °C standing for 3 h. Infections of BMDMs, THP-1-derived human macrophages, and hMDMs with induced strains were performed as described in *SI Appendix, Supplemental Materials and Methods*.

Lactate Dehydrogenase (LDH) Cytotoxicity Assays. After infection, cells were spun at 250 *g* for 10 min to pellet cellular debris. Supernatants were removed and used to assess cytotoxicity via LDH activity. LDH release was quantified using an LDH Cytotoxicity Detection Kit (Roche). Samples were incubated for 25 min at room temperature and absorbance at 490 nm was assessed using a spectrophotometer.

Percent cytotoxicity was calculated after normalizing to uninfected controls and 100% cell death, which is based on 1% triton X-100-treated cells.

ELISA. Supernatants from in vitro infections and murine serum from in vivo infected mice were used to assess IL-1β and IL-18 levels, respectively. For murine IL-1β and IL-18, ELISAs were performed as described in *SI Appendix, Supplemental Materials and Methods*. For measuring human IL-1β, an ELISA kit from BD Biosciences was used.

Immunoblot Analysis. Cellular lysate and supernatant samples were harvested and processed as described in *SI Appendix, Supplemental Materials and Methods*. Samples were resolved on NuPAGE 4 to 12% Bis-Tris precast gels (Invitrogen) followed by transfer to 0.2 μm Polyvinylidene Fluoride membrane (EMD Millipore) at 30 V for 1 h using an XCell SureLock Mini-Cell electrophoresis system (Invitrogen). The following primary antibodies were used for immunoblot analysis: 1:5,000 anti-β-Actin (Sigma clone AC-74), 1:500 anti-Caspase-1 (Genentech), 1:1,000 anti-GSDMD (Abcam [EPR19828]), 1:1,000 anti-mouse NLRC4 (Abcam [EPR19733]), 1:1,000 anti-human NLRC4 (Cell Signaling Technology, clone D5Y8E), 1:1,000 phospho-p38 (Invitrogen, clone C.7.8), and 1:1,000 p38 (Invitrogen, clone p38-3F11). After primary antibody incubation and wash steps, membranes were incubated with species-specific HRP-conjugated secondary antibodies and developed using Pierce ECL Plus (Thermo) or SuperSignal West Femto Maximum Sensitivity Substrate (Thermo) according to the manufacturer's instructions and visualized on a Bio-Rad Gel-Doc XR+ system. Immunoblots were processed and quantified using Image Lab software (Bio-Rad).

In vitro secretion of YopE fusion proteins via the *Yersinia* T3SS was assessed by inducing T3SS expression of indicated strains as described above. Cells were pelleted and proteins in the supernatant were precipitated with trichloroacetic acid (TCA) at 4 °C overnight. The protein pellet was washed with acetone and reconstituted in sample buffer. Samples were run in NuPAGE 4 to 12% Bis-Tris precast gels (Invitrogen), then stained using GelCode Blue Stain Reagent (Thermo Scientific) according to manufacturer instructions.

qRT-PCR. RNA was isolated using TRIzol reagent (ThermoFisher) from either 5×10^6 BMDMs or THP-1s following the manufacturer's protocol. complementary DNA (cDNA) was prepared from the RNA samples using the high-capacity cDNA reverse transcription kit (Applied Biosystems) per the manufacturer's protocol. qPCR was conducted with the QuantBio Studio 6 Flex Real-Time PCR system using the PerfeCTa SYBR Green SuperMix (QuantaBio). For analysis, mRNA levels of siRNA-treated cells were normalized to housekeeping gene *GAPDH* (murine) or *HPRT* (human), and fold induction was determined using the $2^{-\Delta\Delta CT}$ (cycle threshold) method (63). All primers used are listed in *SI Appendix*, Table S1.

Overexpression of NLRC4 in Immortalized Macrophages. WT and *Nlrc4*$^{-/-}$ murine myeloid progenitors were immortalized using the ER-HoxB8 system (64). Murine and human NLRC4 were overexpressed in immortalized *Nlrc4*$^{-/-}$ murine myeloid progenitors as described in *SI Appendix, Supplemental Materials and Methods*. Expression of murine or human NLRC4 in the immortalized myeloid progenitors was verified via immunoblot prior to use. THP-1 hMDMs transduced with the MigR1 retroviral vector alone or overexpressing *hNLRC4* were previously described (65).

Generation of *S.* Tm *Δfljb::kan fliC*^{R475QG}. To mutate SL1344 to express flagellin terminating in a glutamine–glycine in place of arginine, allelic exchange using the suicide vector pCVD442 was performed as described in *SI Appendix, Supplemental Materials and Methods*. The resulting mutant strain *S.* Tm *Δfljb::kan fliC*^{R475QG} was sequence-verified to verify that the desired mutation was present.

Ex Vivo Infections. Two days after intraperitoneal injection of 10- to 12-wk-old C57BL/6J male and/or female mice with 2×10^7 colony forming unit (CFU) of heat-killed *S.* Tm or PBS, peritoneal cells were isolated by peritoneal lavage with 7 mL of sterile PBS. Samples were spun for 5 min at 1,500 rpm at 4 °C. Cells were then resuspended in DMEM with 10 % (vol/vol) FBS and washed a total of three times. 1×10^5 total peritoneal cells per well were plated in 80 μL of DMEM with 10% (vol/vol) FBS and incubated for 3 to 5 h to let the cells adhere to the plate. Prior to infecting with bacteria, the peritoneal cells were washed one time with DMEM containing 10 % (vol/vol) FBS.

In Vivo Infections. 8- to 10-wk-old C57BL/6J male and/or female mice were infected intraperitoneally with SL1344 *Δfljb::kan* and *S.* Tm *Δfljb::kan fliC*^{R475QG} at an inoculum of 500 CFU per mouse in 100 μL PBS. Serum and spleen samples were harvested 2 d postinfection. Serum was used to assay for IL-18 using the ELISA as described above. The spleen was homogenized in 1 mL PBS and plated to assess CFUs.

Statistical Analysis. Graphing and statistical analyses of data were performed using Prism 9 software (GraphPad). Statistical significance was determined using the statistical tests indicated in each figure legend. Differences were considered statistically significant if the *P* value was less than or equal to 0.05.

Data, Materials, and Software Availability. All study data are included in the article and/or *SI Appendix*. Raw data is available at Dryad (66)

ACKNOWLEDGMENTS. We would like to thank Dr. Thirumala-Devi Kanneganti (St. Jude Children's Research Hospital) for *Naip5*$^{-/-}$ bone marrow, Dr. Dieter Schifferli (University of Pennsylvania) for the EPEC strain, Dr. Annelise Snyder for initial flagellin constructs, members of the Shin and Brodsky labs for scientific discussion, Dr. Alex Hoffmann (University of California, Los Angeles) for scientific discussion, and Dr. Patrick Mitchell (University of Washington Seattle) for scientific discussion and critical reading. These studies were supported by NIH grants AI128520, AI139102, AI163596 (I.E.B.), AI123243, AI118861, AI151476 (S.S.), F32AI164655 (J.P.G.), and R01HD098428 (S.W.C.), NSF Graduate Research Fellowship DGE-1321851 (M.S.E.), the Mark Foundation Center for Radiobiology and Immunology (I.E.B., A.J.M.), and Investigators in the Pathogenesis of Infectious Disease Awards from the Burroughs Wellcome Fund (S.S. and I.E.B.).

Author affiliations: [a]Department of Pathobiology, University of Pennsylvania School of Veterinary Medicine, Philadelphia, PA 19104; [b]Department of Microbiology, University of Pennsylvania Perelman School of Medicine, Philadelphia, PA 19104; [c]Department of Pediatrics, Division of Rheumatology, Children's Hospital of Philadelphia, Philadelphia, PA 19104; [d]Department of Radiation Oncology, University of Pennsylvania Perelman School of Medicine, Philadelphia, PA 19104; [e]Abramson Family Cancer Research Institute, University of Pennsylvania Perelman School of Medicine, Philadelphia, PA 19104; [f]Parker Institute for Cancer Immunotherapy, University of Pennsylvania Perelman School of Medicine, Philadelphia, PA 19104; and [g]Mark Foundation Center for Immunotherapy, Immune Signaling, and Radiation, University of Pennsylvania Perelman School of Medicine, Philadelphia, PA 19104

Author contributions: J.P.G., S.S., and I.E.B. designed research; J.P.G., L.L., M.S.E., E.A., and M.A.W.-D. performed research; S.W.C. and S.S. contributed new reagents/analytic tools; J.P.G., L.L., M.S.E., E.A., and S.S. analyzed data; and J.P.G., L.L., A.J.M., and I.E.B. wrote the paper.

1. R. Medzhitov, C. A. Janeway Jr., Decoding the patterns of self and nonself by the innate immune system. *Science* **296**, 298–300 (2002).
2. C. A. Janeway Jr., R. Medzhitov, Innate immune recognition. *Annu. Rev. Immunol.* **20**, 197–216 (2002).
3. C. A. Janeway Jr., Approaching the asymptote? Evolution and revolution in immunology. *Cold Spring Harb. Symp. Quant. Biol.* **54**, 1–13 (1989).
4. Y. H. Sun, H. G. Rolan, R. M. Tsolis, Injection of flagellin into the host cell cytosol by Salmonella enterica serotype Typhimurium. *J. Biol. Chem.* **282**, 33897–33901 (2007).
5. F. Martinon, K. Burns, J. Tschopp, The inflammasome: A molecular platform triggering activation of inflammatory caspases and processing of proIL-beta. *Mol. Cell* **10**, 417–426 (2002).
6. E. M. Kofoed, R. E. Vance, Innate immune recognition of bacterial ligands by NAIPs determines inflammasome specificity. *Nature* **477**, 592–595 (2011).
7. Y. Zhao *et al.*, The NLRC4 inflammasome receptors for bacterial flagellin and type III secretion apparatus. *Nature* **477**, 596–600 (2011).
8. J. Yang, Y. Zhao, J. Shi, F. Shao, Human NAIP and mouse NAIP1 recognize bacterial type III secretion needle protein for inflammasome activation. *Proc. Natl. Acad. Sci. U.S.A.* **110**, 14408–14413 (2013).
9. A. B. Molofsky *et al.*, Cytosolic recognition of flagellin by mouse macrophages restricts Legionella pneumophila infection. *J. Exp. Med.* **203**, 1093–1104 (2006).
10. E. A. Miao *et al.*, Innate immune detection of the type III secretion apparatus through the NLRC4 inflammasome. *Proc. Natl. Acad. Sci. U.S.A.* **107**, 3076–3080 (2010).
11. M. Rayamajhi, D. E. Zak, J. Chavarria-Smith, R. E. Vance, E. A. Miao, Cutting edge: Mouse NAIP1 detects the type III secretion system needle protein. *J. Immunol.* **191**, 3986–3989 (2013).
12. T. Ren, D. S. Zamboni, C. R. Roy, W. F. Dietrich, R. E. Vance, Flagellin-deficient *Legionella* mutants evade caspase-1- and Naip5-mediated macrophage immunity. *PLoS Pathog.* **2**, e18 (2006).
13. I. Rauch *et al.*, NAIP proteins are required for cytosolic detection of specific bacterial ligands in vivo. *J. Exp. Med.* **213**, 657–665 (2016).
14. T. Grandjean *et al.*, The human NAIP-NLRC4-inflammasome senses the Pseudomonas aeruginosa T3SS inner-rod protein. *Int. Immunol.* **29**, 377–384 (2017).

15. J. Kortmann, S. W. Brubaker, D. M. Monack, Cutting edge: Inflammasome activation in primary human macrophages is dependent on Flagellin. *J. Immunol.* **195**, 815–819 (2015).
16. N. Naseer *et al.*, Human NAIP/NLRC4 and NLRP3 inflammasomes detect Salmonella type III secretion system activities to restrict intracellular bacterial replication. *PLoS Pathog.* **18**, e1009718 (2022).
17. V. M. Reyes Ruiz *et al.*, Broad detection of bacterial type III secretion system and flagellin proteins by the human NAIP/NLRC4 inflammasome. *Proc. Natl. Acad. Sci. U.S.A.* **114**, 13242–13247 (2017).
18. S. Mariathasan *et al.*, Differential activation of the inflammasome by caspase-1 adaptors ASC and Ipaf. *Nature* **430**, 213–218 (2004).
19. Z. Hu *et al.*, Structural and biochemical basis for induced self-propagation of NLRC4. *Science* **350**, 399–404 (2015).
20. L. Franchi *et al.*, Cytosolic flagellin requires Ipaf for activation of caspase-1 and interleukin 1beta in salmonella-infected macrophages. *Nat. Immunol.* **7**, 576–582 (2006).
21. C. A. Diebolder, E. F. Halff, A. J. Koster, E. G. Huizinga, R. I. Koning, Cryoelectron tomography of the NAIP5/NLRC4 inflammasome: Implications for NLR activation. *Structure* **23**, 2349–2357 (2015).
22. D. S. Zamboni *et al.*, The Birc1e cytosolic pattern-recognition receptor contributes to the detection and control of Legionella pneumophila infection. *Nat. Immunol.* **7**, 318–325 (2006).
23. E. A. Miao *et al.*, Cytoplasmic flagellin activates caspase-1 and secretion of interleukin 1beta via Ipaf. *Nat. Immunol.* **7**, 569–575 (2006).
24. P. Li *et al.*, Mice deficient in IL-1 beta-converting enzyme are defective in production of mature IL-1 beta and resistant to endotoxic shock. *Cell* **80**, 401–411 (1995).
25. K. Kuida *et al.*, Altered cytokine export and apoptosis in mice deficient in interleukin-1 beta converting enzyme. *Science* **267**, 2000–2003 (1995).
26. J. Shi *et al.*, Cleavage of GSDMD by inflammatory caspases determines pyroptotic cell death. *Nature* **526**, 660–665 (2015).
27. L. A. Cummings, W. D. Wilkerson, T. Bergsbaken, B. T. Cookson, In vivo, fliC expression by Salmonella enterica serovar Typhimurium is heterogeneous, regulated by ClpX, and anatomically restricted. *Mol. Microbiol.* **61**, 795–809 (2006).
28. E. A. Miao *et al.*, Caspase-1-induced pyroptosis is an innate immune effector mechanism against intracellular bacteria. *Nat. Immunol.* **11**, 1136–1142 (2010).
29. A. Hausmann *et al.*, Intestinal epithelial NAIP/NLRC4 restricts systemic dissemination of the adapted pathogen Salmonella Typhimurium due to site-specific bacterial PAMP expression. *Mucosal. Immunol.* **13**, 530–544 (2020).
30. S. Saini, J. M. Slauch, P. D. Aldridge, C. V. Rao, Role of cross talk in regulating the dynamic expression of the flagellar Salmonella pathogenicity island 1 and type 1 fimbrial genes. *J. Bacteriol.* **192**, 5767–5777 (2010).
31. M. K. Stewart, L. A. Cummings, M. L. Johnson, A. B. Berezow, B. T. Cookson, Regulation of phenotypic heterogeneity permits Salmonella evasion of the host caspase-1 inflammatory response. *Proc. Natl. Acad. Sci. U.S.A.* **108**, 20742–20747 (2011).
32. P. S. Mitchell *et al.*, NAIP–NLRC4-deficient mice are susceptible to shigellosis. *Elife* **9**, e59022 (2020).
33. J. L. Roncaioli *et al.*, A hierarchy of cell death pathways confers layered resistance to shigellosis in mice. *Elife* **12**, e83639 (2023).
34. K. Yonekura, S. Maki-Yonekura, K. Namba, Complete atomic model of the bacterial flagellar filament by electron cryomicroscopy. *Nature* **424**, 643–650 (2003).
35. J. L. Tenthorey *et al.*, The structural basis of flagellin detection by NAIP5: A strategy to limit pathogen immune evasion. *Science* **358**, 888–893 (2017).
36. K. L. Lightfield *et al.*, Critical function for Naip5 in inflammasome activation by a conserved carboxy-terminal domain of flagellin. *Nat. Immunol.* **9**, 1171–1178 (2008).
37. X. Yang *et al.*, Structural basis for specific flagellin recognition by the NLR protein NAIP5. *Cell Res.* **28**, 35–47 (2018).
38. J. Yang *et al.*, Sequence determinants of specific pattern-recognition of bacterial ligands by the NAIP–NLRC4 inflammasome. *Cell Discov.* **4**, 22 (2018).
39. L. Zhang *et al.*, Cryo-EM structure of the activated NAIP2–NLRC4 inflammasome reveals nucleated polymerization. *Science* **350**, 404–409 (2015).
40. F. G. Bauernfeind *et al.*, Cutting edge: NF-kappaB activating pattern recognition and cytokine receptors license NLRP3 inflammasome activation by regulating NLRP3 expression. *J. Immunol.* **183**, 787–791 (2009).
41. T. Henry, A. Brotcke, D. S. Weiss, L. J. Thompson, D. M. Monack, Type I interferon signaling is required for activation of the inflammasome during Francisella infection. *J. Exp. Med.* **204**, 987–994 (2007).
42. X. Dong *et al.*, Brd4 regulates NLRC4 inflammasome activation by facilitating IRF8-mediated transcription of Naips. *J. Cell Biol.* **220**, e202005148 (2021).
43. R. Karki *et al.*, IRF8 regulates transcription of naips for NLRC4 inflammasome activation. *Cell* **173**, 920–933.e13 (2018).
44. J. D. Sauer *et al.*, Listeria monocytogenes engineered to activate the Nlrc4 inflammasome are severely attenuated and are poor inducers of protective immunity. *Proc. Natl. Acad. Sci. U.S.A.* **108**, 12419–12424 (2011).
45. V. Kapatral, J. W. Olson, J. C. Pepe, V. L. Miller, S. A. Minnich, Temperature-dependent regulation of Yersinia enterocolitica Class III flagellar genes. *Mol. Microbiol.* **19**, 1061–1071 (1996).
46. T. H. Chen, S. S. Elberg, Scanning electron microscopic study of virulent Yersinia pestis and Yersinia pseudotuberculosis type 1. *Infect. Immun.* **15**, 972–977 (1977).
47. L. W. Peterson *et al.*, RIPK1-dependent apoptosis bypasses pathogen blockade of innate signaling to promote immune defense. *J. Exp. Med.* **214**, 3171–3182 (2017).
48. D. Weng *et al.*, Caspase-8 and RIP kinases regulate bacteria-induced innate immune responses and cell death. *Proc. Natl. Acad. Sci. U.S.A.* **111**, 7391–7396 (2014).
49. N. H. Philip *et al.*, Caspase-8 mediates caspase-1 processing and innate immune defense in response to bacterial blockade of NF-kappaB and MAPK signaling. *Proc. Natl. Acad. Sci. U.S.A.* **111**, 7385–7390 (2014).
50. I. E. Brodsky *et al.*, A Yersinia effector protein promotes virulence by preventing inflammasome recognition of the type III secretion system. *Cell Host Microbe* **7**, 376–387 (2010).
51. L. Franchi, T. Eigenbrod, G. Nunez, Cutting edge: TNF-alpha mediates sensitization to ATP and silica via the NLRP3 inflammasome in the absence of microbial stimulation. *J. Immunol.* **183**, 792–796 (2009).
52. M. Doerflinger *et al.*, Flexible usage and interconnectivity of diverse cell death pathways protect against intracellular infection. *Immunity* **53**, 533–547.e7 (2020).
53. P. Broz *et al.*, Redundant roles for inflammasome receptors NLRP3 and NLRC4 in host defense against Salmonella. *J. Exp. Med.* **207**, 1745–1755 (2010).
54. R. K. Wilson, R. K. Shaw, S. Daniell, S. Knutton, G. Frankel, Role of EscF, a putative needle complex protein, in the type III protein translocation system of enteropathogenic Escherichia coli. *Cell Microbiol.* **3**, 753–762 (2001).
55. K. A. Lord, B. Hoffman-Liebermann, D. A. Liebermann, Nucleotide sequence and expression of a cDNA encoding MyD88, a novel myeloid differentiation primary response gene induced by IL6. *Oncogene* **5**, 1095–1097 (1990).
56. L. M. Jenster *et al.*, P38 kinases mediate NLRP1 inflammasome activation after ribotoxic stress response and virus infection. *J. Exp. Med.* **220**, e20220837 (2023).
57. G. Fenini *et al.*, The p38 mitogen-activated protein kinase critically regulates human keratinocyte inflammasome activation. *J. Invest. Dermatol.* **138**, 1380–1390 (2018).
58. M. S. Stratton *et al.*, Dynamic chromatin targeting of BRD4 stimulates cardiac fibroblast activation. *Circ. Res.* **125**, 662–677 (2019).
59. Y. Qu *et al.*, NLRP3 recruitment by NLRC4 during Salmonella infection. *J. Exp. Med.* **213**, 877–885 (2016).
60. J. L. Tenthorey *et al.*, NLRC4 inflammasome activation is NLRP3- and phosphorylation-independent during infection and does not protect from melanoma. *J. Exp. Med.* **217**, e20191736 (2020).
61. P. Schnupf, P. J. Sansonetti, Shigella pathogenesis: New insights through advanced methodologies. *Bacteria and Intracellularity* 15–39 (2019).
62. E. F. Halff *et al.*, Formation and structure of a NAIP5-NLRC4 inflammasome induced by direct interactions with conserved N- and C-terminal regions of flagellin. *J. Biol. Chem.* **287**, 38460–38472 (2012).
63. K. J. Livak, T. D. Schmittgen, Analysis of relative gene expression data using real-time quantitative PCR and the 2(-Delta Delta C(T)) Method. *Methods* **25**, 402–408 (2001).
64. G. G. Wang *et al.*, Quantitative production of macrophages or neutrophils ex vivo using conditional Hoxb8. *Nat. Methods* **3**, 287–293 (2006).
65. S. W. Canna *et al.*, An activating NLRC4 inflammasome mutation causes autoinflammation with recurrent macrophage activation syndrome. *Nat. Genet.* **46**, 1140–1146 (2014).
66. J. Grayczyk *et al.*, TLR priming licenses NAIP inflammasome activation by immunoevasive ligands. Dryad. https://doi.org/10.5061/dryad.fj6q57443. Deposited 4 November 2024.